International Journal of Bifurcation and Chaos

HYPERBOLIC CHAOS AND OTHER PHENOMENA OF COMPLEX DYNAMICS DEPENDING ON PARAMETERS IN A NON-AUTONOMOUS SYSTEM OF TWO ALTERNATELY ACTIVATED OSCILLATORS

OLGA B. ISAEVA
Kotel'nikov's Institute of Radio-Engineering and Electronics of RAS, Saratov Branch
Zelenaya 38, Saratov, 410019, Russian Federation
Department of Nonlinear Processes, Chernyshevsky Saratov State University
Astrakhanskaya 83, Saratov, 410012, Russian Federation
isaevao@rambler.ru

SERGEY P. KUZNETSOV
Kotel'nikov's Institute of Radio-Engineering and Electronics of RAS, Saratov Branch
Zelenaya 38, Saratov, 410019, Russian Federation
Department of Nonlinear Processes, Chernyshevsky Saratov State University
Astrakhanskaya 83, Saratov, 410012, Russian Federation
spkuz@yandex.ru

IGOR R. SATAEV
Kotel'nikov's Institute of Radio-Engineering and Electronics of RAS, Saratov Branch
Zelenaya 38, Saratov, 410019, Russian Federation
sataevir@rambler.ru

DMITRY V. SAVIN
Department of Nonlinear Processes, Chernyshevsky Saratov State University
Astrakhanskaya 83, Saratov, 410012, Russian Federation
savin.dmitry.v@gmail.com

EUGENE P. SELEZNEV
Kotel'nikov's Institute of Radio-Engineering and Electronics of RAS, Saratov Branch
Zelenaya 38, Saratov, 410019, Russian Federation
Department of Nano- and Biomedical Techology, Chernyshevsky Saratov State University
Astrakhanskaya 83, Saratov, 410012, Russian Federation
evgenii_seleznev@mail.ru

Received (to be inserted by publisher)

We provide a multi-parameter analysis of dynamics in a non-autonomous system of two alternately exciting self-oscillatory elements able to demonstrate a uniformly chaotic attractor of Smale–Williams type in the stroboscopic Poincaré map. Parameter space charts of regular and chaotic regimes are presented. Possible scenarios of the onset of hyperbolic chaos are discussed. The numerical studies are supplemented by experimental results obtained for a laboratory electronic device.

Keywords: strange attractor, chaos, hyperbolic chaos, Smale–Williams solenoid, scenario of transition to chaos

Introduction

In the oscillation theory one of the basic principles both for formal analysis and for practical applications is priority of considering and using rough systems, whose dynamical properties are insensitive in respect to small variations of parameters and functions in the governing equations [Andronov & Pontryagin, 1937; Andronov *et al.*, 1966]. If we talk about chaotic systems, the property of roughness, rigorously formalized in the modern theory of dynamical systems as structural stability [Anosov, 1995; Katok & Hasselblatt, 1997; Shil'nikov *et al.*, 1998, 2001; Afraimovich & Hsu, 2003], is inherent exclusively to the hyperbolic chaos. In the context of conservative dynamics it occurs in Anosov systems [Anosov, 1967, 1995; Katok & Hasselblatt, 1997], and in the dissipative dynamics in systems with uniformly hyperbolic attractors [Smale, 1967; Anosov, 1995; Katok & Hasselblatt, 1997; Afraimovich & Hsu, 2003]. In view of the above mentioned common principle, it looks odd and paradoxical that for a long time examples of the hyperbolic chaotic attractors were known only as mathematical constructions, like Smale–Williams solenoid [Smale, 1967; Williams, 1974; Devaney, 1989; Shil'nikov, 1997], Plykin attractor [Plykin, 1974; Devaney, 1989; Zhirov, 2000], DA-attractor of Smale [Smale, 1967; Devaney, 1989; Shil'nikov, 1997], without any natural application. Physically implementable systems with such attractors have been discovered (or rather, constructed) only recently [Hunt, 2001; Hunt & MacKay, 2003; Belykh *et al.*, 2005; Kuznetsov, 2005, 2011a, 2012; Isaeva *et al.*, 2006, 2011; Kuznetsov & Pikovsky, 2007]. Beside the differential equations studied by means of numeric computations, some electronic devices with hyperbolic attractors were elaborated; their operation was demonstrated in circuit simulations [Kuznetsov, 2011b,c; Kuznetsov *et al.*, 2013] and in real experiments [Kuznetsov & Seleznev, 2006; Kuznetsov & Ponomarenko, 2008; Baranov *et al.*, 2010; Kuznetsov *et al.*, 2013]. So, now one can talk about formation of a background for possible applications of the structurally stable chaos, for example, in secure communication [Dmitriev & Panas, 2002; Yang, 2004; Koronovskii *et al.*, 2009; Dmitriev *et al.*, 2012], in noise radar technologies [Lukin, 2001; Liu *et al.*, 2011], in cryptography [Baptista, 1998; Zhen *et al.*, 2014], for generating random numbers [Stojanovski & Kocarev, 2001; Stojanovski *et al.*, 2001; Elwakil, 2002]. The main advantage of devices with hyperbolic chaos from a practical point of view will be insensitivity of characteristics of generated chaotic signals to nuisance factors, like manufacturing errors, noise, interferences, etc. Moreover, it may be expected that the well-developed rigorous mathematical theory of hyperbolic chaos can provide a solid foundation for applications in some non-trivial aspects. Say, a possibility of perfect representation of the hyperbolic dynamics in terms of symbolic sequences of a finite alphabet [Devaney, 1989; Katok & Hasselblatt, 1997; Shil'nikov, 1997; Afraimovich & Hsu, 2003] appears to be in obvious direct correspondence with ideology and content of the information and communication theory [Shannon, 1948].

Both from theoretical point of view and for practical elaboration of systems producing the hyperbolic chaos, a question is important concerning scenarios of origin of the uniformly hyperbolic attractors in the course of variation of one or more control parameters. Note that this issue is certainly different from the traditional collection of roads to chaos, which concerns formation of non-hyperbolic attractors, like that of Feigenbaum [Eckmann, 1981; Feigenbaum, 1983; Bergé *et al.*, 1984; Schuster & Just, 2005].

In the context of the onset of turbulence possible occurrence of hyperbolic chaotic attractors was discussed four decades ago by Ruelle and Takens [Ruelle & Takens, 1971; Newhouse *et al.*, 1978], but they did not consider any concrete example of dynamical equations demonstrating the phenomenon. Shil'nikov & Turaev [1997] have advanced a scenario of formation of the Smale–Williams attractor in a kind of the so-called blue sky catastrophe; an explicit example was suggested later [Kuznetsov, 2010]. One more scenario for the onset or destruction of the Smale–Williams attractor [Isaeva *et al.*, 2012, 2013] is associated with a collision of two chaotic invariant sets, an attracting solenoid and a non-attracting one.

The question of examination and classification of scenarios of emergence of any dynamical phenomenon, say, of the hyperbolic chaos, may be reformulated as a problem of exploration of arrangement of the pa-

rameter space of a representative dynamical system in domains adjacent to the region of occurrence of the phenomenon. For the hyperbolic chaos itself, the domain of its existence is expected to be structureless because of its roughness, but description of generic configurations of surrounding regions, their mutual disposition in the parameter space, and relevant bifurcations deserve consideration. For investigation of these issues it is appropriate to apply tools and concepts elaborated and used in modern computational nonlinear dynamics, including graphical presentation of attractors, charts of dynamical regimes in parameter space, analysis of Lyapunov exponents, and so on.

The article is devoted to exploration of the dynamical behavior depending on parameters for a particular non-autonomous system with hyperbolic attractor proposed originally by Kuznetsov [2005]. The system is composed of two self-oscillatory elements, which become active turn by turn due to the externally supplied parameter modulation, and transfer the excitation each other in such way that the double expanding transformation of phases of the oscillations takes place on each time interval of the modulation period. Attractor of the stroboscopic Poincaré map is a kind of Smale–Williams solenoid, and this assertion was verified in computations by testing conditions of hyperbolicity with several independent approaches [Kuznetsov & Sataev, 2006, 2007; Wilczak, 2010; Kuptsov, 2012]. To make the analysis comprehensive as far as possible, the system is modified comparing with the original version by introducing some additional control parameters. Beside the computational data we discuss experiments with a specially designed and built laboratory electronic device.

1. Smale–Williams attractor and the basic equations

To start, let us remind the classic mathematical construction of the Smale–Williams solenoid, which is conceptually the simplest example of a uniformly hyperbolic chaotic attractor and can occur in discrete time dynamics in a state space of dimension three or more. Consider a domain in a form of a torus in the three-dimensional state space. Suppose that on one step of the mapping we stretch the object twice squeezing it in the transversal direction, fold it to get the double loop, and insert this loop within the original torus, as shown in Fig. 1. At each next repetition of the transformation the total volume decreases (that means the map is dissipative) and the number of coils is doubled. In the limit we get the solenoid with infinite number of coils and with subtle Cantor-like structure in transversal cross-section. The essential point of the construction is that the angular coordinate counted around the torus undergoes doubling at each discrete time step: $\varphi^{n+1} = 2\varphi^n + \text{const}$. Hence, the attractor is chaotic: this double expanding circle map, or a Bernoulli map, manifests chaos characterized by the positive Lyapunov exponent $\Lambda = \ln 2$.

Hereafter we explore a physically realizable system, which is defined by a set of differential equations

$$\begin{aligned} &\ddot{x} - (h_1 + A_1\cos(2\pi t/T) - x^2)\dot{x} + {\omega_0}^2 x = \varepsilon_1 y\cos\omega t, \\ &\ddot{y} - (h_2 - A_2\cos(2\pi t/T) - y^2)\dot{y} + (2\omega_0)^2 x = \varepsilon_2 x^2. \end{aligned} \tag{1}$$

This is a modified version of the model of [Kuznetsov, 2005] composed of two subsystems, the van der Pol oscillators with characteristic frequencies ω_0 and $2\omega_0$. The variables x and y are the generalized coordinates of the oscillators. The parameter responsible for the limit cycle birth is forced to vary slowly in opposite phases in one and other subsystem with period T and amplitudes A_1 and A_2 around the mean values h_1 and h_2, which will be referred to as the mean activity control parameters. Due to the modulation, the subsystems become active or suppressed turn by turn. The coupling of the subsystems is characterized by coefficients ε_1 and ε_2.

The ratio $\omega T/2\pi$ is supposed to be integer; hence, the dynamics may be treated in terms of the four-dimensional stroboscopic Poincaré map $\mathbf{x}^{n+1} = \mathbf{T}(\mathbf{x}^n)$ determined on successive time intervals of duration T for the state vectors $\mathbf{x}^n = \{x(nT), \dot{x}(nT), y(nT), \dot{y}(nT)\}$. Practically, the Poincaré map can be implemented as a computational routine providing integration of the Eq. (1) on a time interval equal to the modulation period.

The system (1) reduces to the original model [Kuznetsov, 2005] if we set $h_1 = h_2 = 0, A_1 = A_2 = A, \varepsilon_1 = \varepsilon_2 = \varepsilon, \omega = \omega_0$. As found, in a wide parameter range the attractor of Smale–Williams type occurs in the state space of the Poincaré map. Fig. 2 illustrates chaotic dynamics associated with the Smale–Williams attractor at $A = 3.0, T = 10, \varepsilon = 0.5, \omega = 2\pi$. Panel (a) shows the time dependences for the variables of two

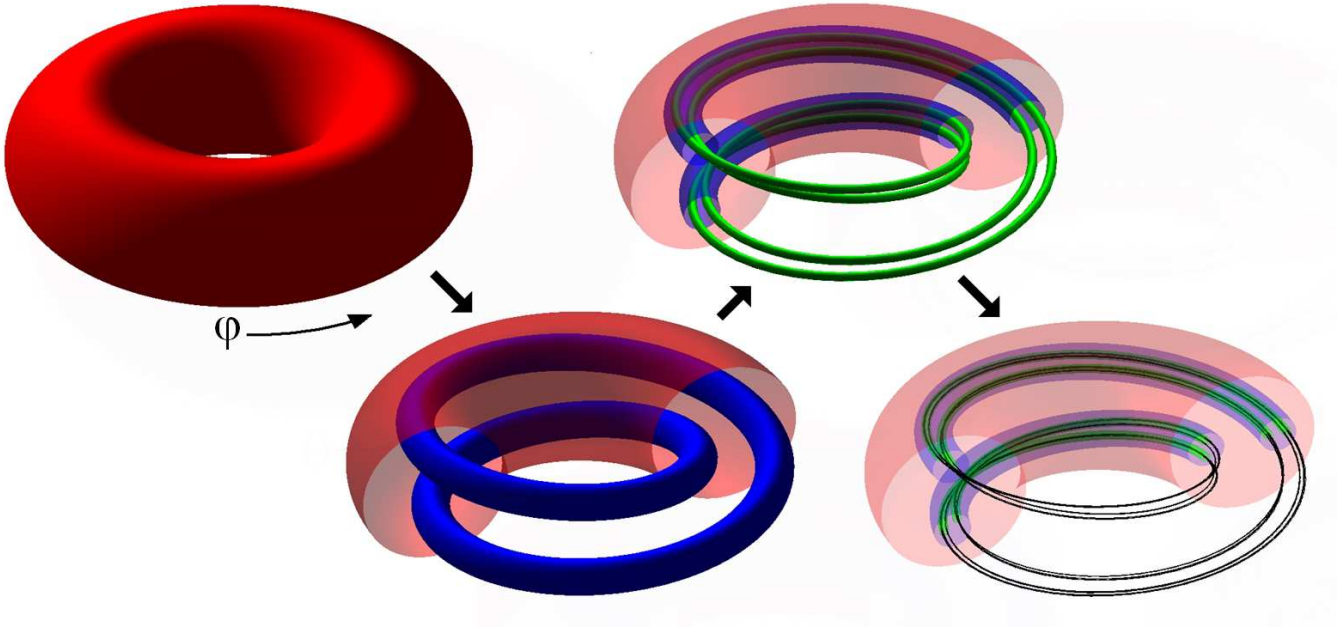

Fig. 1. Classic construction of the Smale–Williams attractor: initial toroidal domain in three-dimensional state space, results of its transformation in the first two iterations of the mapping, and the solenoid obtained after a large number of repetitive applications of the procedure. The angular variable φ of any instant state of the system undergoes doubling on each next step of the transformation.

partial subsystems. With alternating excitation and suppression for the first and the second oscillators, the observed sequence of the oscillatory trains is, in fact, chaotic. Chaos exposes itself in variations of phases of the oscillations on successive stages of activity of the subsystems. Panel (b) illustrates time evolution of the phases of the first and second subsystems defined as $\varphi_1 = \arg(x + i\dot{x}/\omega)$ and $\varphi_2 = \arg(y + i\dot{y}/2\omega)$. As seen from panels (c) and (d), these phases considered at successive modulation periods stroboscopically, obey the double-expanding circle map. In good approximation it is the Bernoulli map $\varphi^{n+1} = 2\varphi^n + \text{const}$; as known, it is chaotic and characterized by positive Lyapunov exponent $\Lambda = \ln 2$. Respective phase portraits of attractors of the Poincaré map projected on the plane of the generalized coordinates and velocities of the first and second oscillator visualize the Smale–Williams attractor with intrinsic subtle structure of transversal splitting of the filaments (see panels (e), (f)).

Qualitatively, one can explain occurrence of the Smale–Williams attractor as follows. The parameter modulation in one and other subsystem takes place in counter-phase; so, on one half of the modulation period the first oscillator is active and the second is below the excitation threshold and vise versa. The first oscillator acts on the second one via the quadratic term x^2. It contains the second harmonic component, which is resonant with natural oscillations of the second subsystem. So, the second oscillator stimulated in the beginning of its activity stage by the first oscillator accepts the second harmonic phase, which is doubled comparing the original phase of the first oscillator. In turn, the second oscillator at final part of its activity stage acts on the first one by a linear term multiplied by a constant-amplitude reference signal. A component of the difference frequency is resonant for the first oscillator stimulating its excitation on the next stage of activity with inheritance of the phase of the second oscillator, and so on. This consecutive doubling of phases for successively generated oscillatory trains is accompanied with compression of the phase volume in other dimensions in the state space of the Poincaré map, and it corresponds exactly to the formal construction of the Smale–Williams solenoid: formation of a doubled loop as an image of a toroidal domain in the state space with its insertion into the original torus [Kuznetsov & Sataev, 2006, 2007]. The uniformly hyperbolic nature of the attractor in the system under consideration has been confirmed by computational verification of hyperbolicity conditions in a frame of several independent approaches [Kuznetsov & Sataev, 2006, 2007; Wilczak, 2010; Kuptsov, 2012].

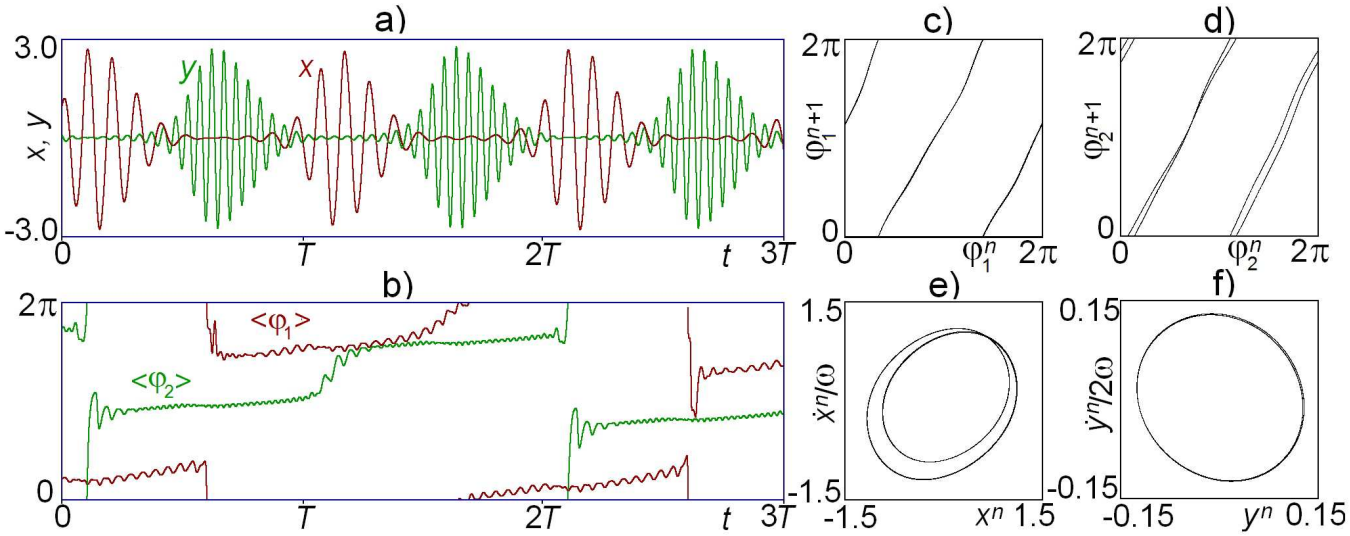

Fig. 2. Graphical representation of oscillations in the first and the second subsystems in time (a). The phases of oscillations in the subsystems averaged over high-frequency characteristic period $\langle\varphi_{1,2}\rangle_{2\pi/\omega}$ versus time (b). Panels (c) and (d) show iteration diagrams for the phases associated with successive activity stages for two oscillators and correspond to the two-fold expanding circle map. Panels (e) and (f) are portraits of attractors in the stroboscopic section. Parameters in the equations (1) are $h_{1,2} = 0, A = 3.0, T = 10, \varepsilon_{1,2} = 0.5, \omega = 2\pi$.

2. Parameter space of the system with hyperbolic chaos

In the parameter space of the system (1), which is extension of the parameter space of the original model [Kuznetsov, 2005], the hyperbolic dynamics associated with the Smale–Williams attractor will occur in some domain, which apparently will be surrounded by regions of distinct types of dynamics, chaotic or regular. The hyperbolic chaos region itself will be structureless because of roughness of the phenomenon. However, on roads in the parameter space, which lead to the hyperbolicity region, one can expect to observe certain scenarios of formation of the hyperbolic chaotic attractor, which should be distinguished and catalogued.

Let us start with the parameter plane chart of the system (1) obtained in computations for the case $h_1 = h_2 = h$ and $A_1 = A_2 = A$. It is shown in Fig. 3 in coordinates (A, h).

To draw the chart we scan the parameter plane on a grid with small finite steps along the coordinate axes. At each point about 10^3 iterations of the Poincaré map are produced, and the largest Lyapunov exponent is evaluated using the Benettin algorithm [Benettin *et al.*, 1980; Schuster & Just, 2005] from joint numerical integration of the equations (1) together with the corresponding variation equations linearized nearby the reference phase trajectory on the attractor. Then, the pixels are colored depending on the computed values of the senior Lyapunov exponent of the Poincaré map. Negative values are indicated by gray tones and correspond to periodic dynamics (P) associated with attracting limit cycles. Black regions designate absence of oscillations in the sustained regime ("oscillation death", OD), i.e. arrival of the system at the trivial attractive fixed point at zero. Red color designates quasiperiodic dynamics (Q) with the Lyapunov exponent equal zero (up to numerical errors). Blue tones correspond to chaotic dynamics characterized by a positive Lyapunov exponent. The hyperbolic chaos (HC) associated with the Smale–Williams attractor is shown in light blue and corresponds to the Lyapunov exponent of the Poincaré map close to the value of $\ln 2$. Region of coexistence of attractors (multistability) is marked by hatching with inclined bands of colors attributed to the respective attractors.

In the left-hand part of the chart, moving upward, with increase of the amplitude modulation parameter A, from the situation of absence of oscillations we come to the region of coexistence of the attractive fixed point in the origin with the hyperbolic Smale–Williams attractor associated with alternating excitation of the subsystems of relatively large amplitude. It corresponds to the "saddle-node" scenario of birth of the

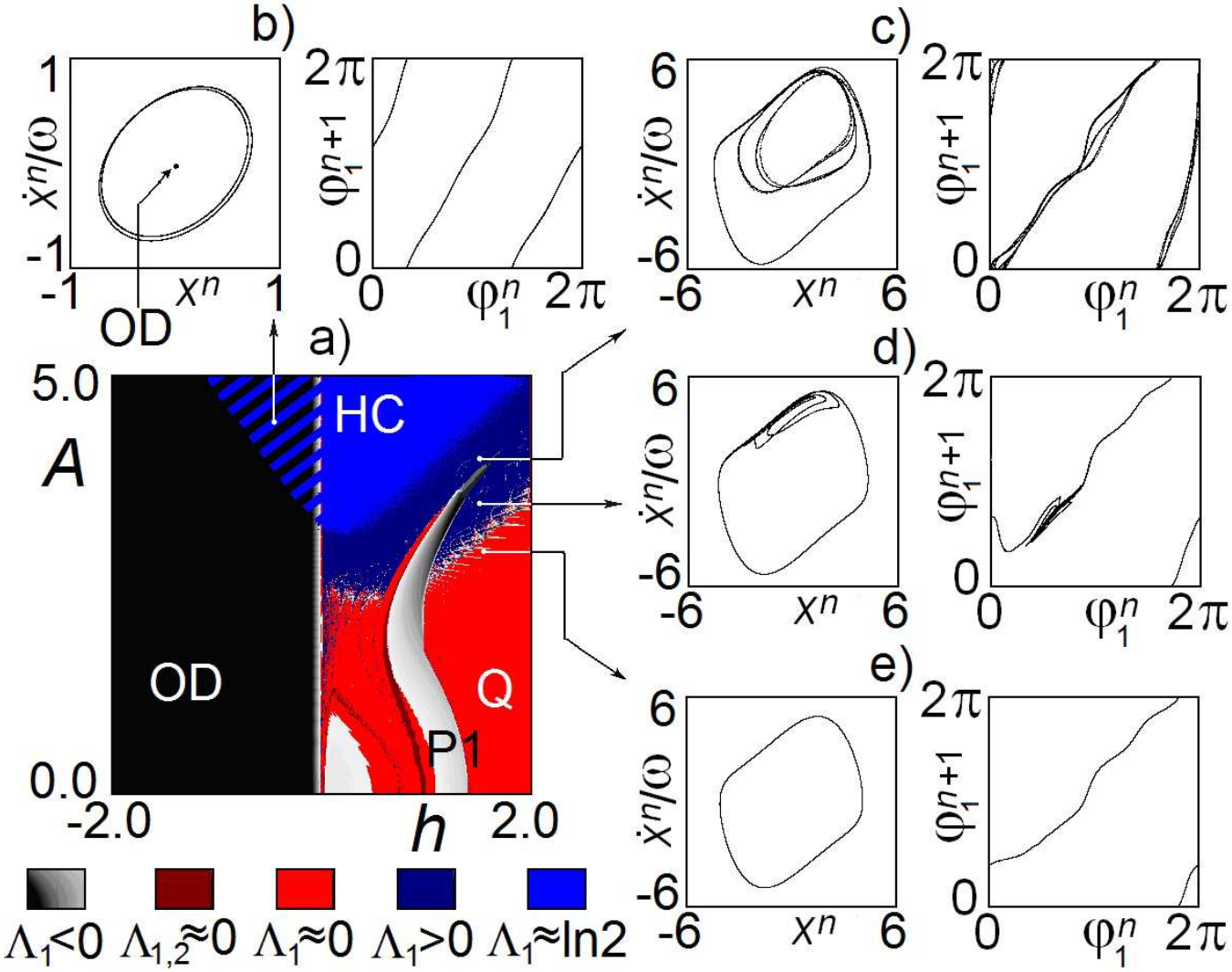

Fig. 3. A chart of regimes on the parameter plane of the model (1) for $h_1 = h_2 = h$ and $A_1 = A_2 = A$ with other parameters $\varepsilon_1 = \varepsilon_2 = 0.5$, $T_2 = 8$, $\omega = 2\pi$ (a). Phase portraits and iteration diagrams for phases of oscillations in one of the subsystems are shown demonstrating coexistence of hyperbolic chaos (HC) with the oscillation death regime (OD) at $h = -0.5$, $A = 4.5$ (b), and formation of the hyperbolic attractor after destruction of a quasi-periodic regime Q associated with the invariant curve at $h = 1.5$, $A = 4.0$ (c), $h = 1.5$, $A = 3.5$ (d), $h = 1.5$, $A = 3.0$ (e).

hyperbolic attractor that we discussed earlier [Isaeva *et al.*, 2012, 2013]. [1]

A richer assortment of dynamical behavior is observed in the right-hand half of the parameter plane diagram, at positive values of h. In the lower part of the chart, each of two individual non-autonomous van der Pol oscillators constituting the system manifests quasi-periodic oscillations that can be synchronized in some parameter regions due to the coupling between the subsystems and the external driving. A domain of quasi-periodicity (Q) is observed here alternating with zones of periodic behavior (P). With increase of the modulation amplitude A at some place the mechanism of excitation transfer starts to work, as described in Section 1, with phase doubling: at some stages of the process the amplitude of one oscillator is large enough and for another it is small enough to provide effective phase transfer from the partner subsystem at each next stage of activity. Transition from quasi-periodic behavior to hyperbolic chaos takes place here

[1] It is interesting to mention a connection of this scenario with some detached chapter of nonlinear dynamics that deals with complex analytic maps and objects like the Mandelbrot and Julia sets; concerning this issue see Refs. [Isaeva *et al.*, 2007, 2008, 2012].

according to some new scenario. In the course of this transition the invariant curve in the Poincaré section associated with the quasi-periodicity undergoes a deformation that corresponds to the loss of reversibility of the function describing transformation of the angular variables, i.e. the phases for successive oscillatory trains. In the phase portraits of the attractors it is accompanied by appearance of "curls". This dynamical regime corresponds to chaos (C), which is not still hyperbolic, and, hence, is not rough. Indeed, on the chart of parameter plane the regularity windows are distinguishable under appropriate resolution. With further increase of parameter A the mapping for phases converts to the double expanding circle map while the portrait of the attractor is transformed to that of the solenoid due to the widening of the mentioned curls. (Compare the pictures (e), (d), and (c).) Surely, this scenario requires further examination, but here we limit ourselves with this short qualitative description.

Now, let us turn to the case when the mean activity control parameters h_1 and h_2 can be regulated independently. Chart of regimes on the parameter plane (h_1, h_2) at the fixed modulation amplitude $A = A_1 = A_2 = 4.0$ is shown in Fig. 4. In panel (a) in the lower left quadrant of the chart we observe decay of oscillations to trivial zero state. In the right top corner of this "black square" the trivial attractor without oscillations coexists with the Smale–Williams attractor that can arise with initial conditions of sufficiently large amplitude. Mechanism of formation of the Smale–Williams attractor corresponds to the above mentioned "saddle-node" scenario [Isaeva *et al.*, 2012, 2013].

Domain of the hyperbolic chaos occupies the central part of the chart of panel (a). With increase of h_1 or h_2 we leave this region: with large one or other activity parameter the modulation of the amplitude becomes insufficient for the phase transfer with doubling; instead we have direct transfer of the phase from the previous stage of activity to the next one, and the dynamics tend to be quasiperiodic instead of that associated with the hyperbolic chaos. From enlarged fragments of the chart shown in panels (b) and (c) one can observe different character of the destruction of the hyperbolic attractor under increase of the mean activity control parameter in the first or second subsystem.

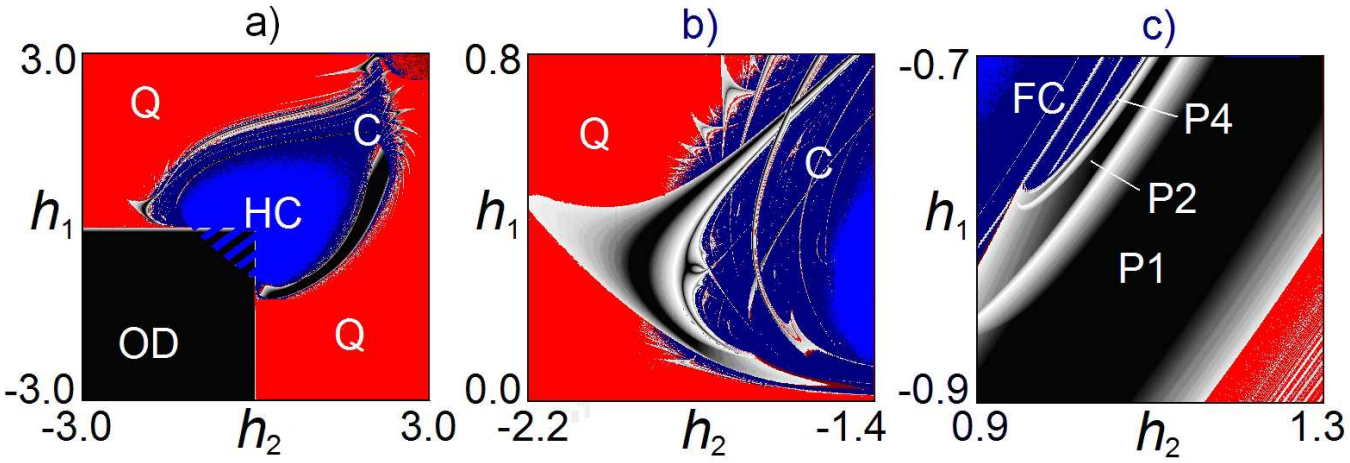

Fig. 4. Chart of dynamical regimes in the parameter plane of mean activity control parameters for the system (1) with $\varepsilon_1 = \varepsilon_2 = 0.5$, $T_2 = 8$, $A = 4.0$ (a), and its enlarged fragments illustrating transitions to hyperbolic chaos through destruction of quasi-periodicity (b) and via the cascade of period doubling of the limit cycles (P1, P2, P4) and the Feigenbaum chaos (FC) (c). Color coding is similar to that of Fig. 3.

Indeed, in the region corresponding to $h_1 > h_2$ (panel (b)) the picture shows a set of synchronization tongues and quasi-periodicity between them. In this case the transition from fractalized torus to the hyperbolic attractor with increase of h_2 is of the same kind as discussed for the right-hand part of the chart of Fig. 3. In contrast, in the region corresponding to $h_1 < h_2$ (panel (c)), with increase of h_1 starting from the quasi-periodicity, we observe, first, appearance of an attractive limit cycle of period 1 due to synchronization on the torus, and then a cascade of period doubling bifurcations resulting in appearance of a non-rough chaotic attractor referred to as the Feigenbaum chaos (FC); afterward it is transformed into

the hyperbolic attractor.

Occurrence of two different scenarios “torus — hyperbolic attractor” and “period-doubling — Feigenbaum attractor — hyperbolic chaos” reflects asymmetry between two partial oscillatory elements constituting the system due to different nature of coupling terms responsible for transfer of the excitation from the first to the second oscillator and back, respectively, the quadratic and linear terms. To clarify the question let us turn to Fig. 5, which shows the chart of regimes on the plane of the coupling coefficients ε_1 and ε_2 supplemented with a set of characteristic phase portraits and iteration diagrams for the phases.

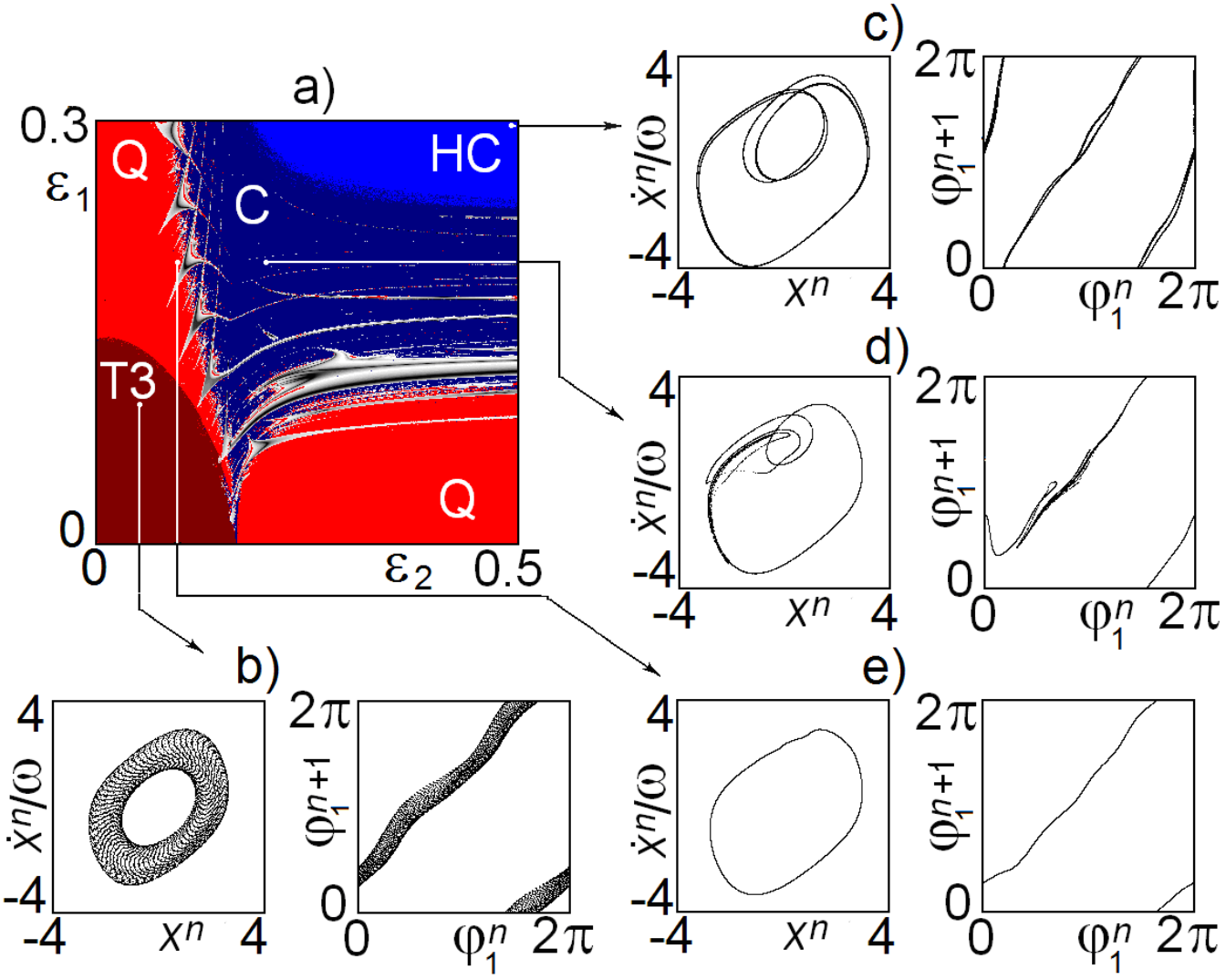

Fig. 5. Chart of dynamical regimes of the system (1) with $A = 4.0$, $h_1 = h_2 = 1.0$ in the plane of the coupling coefficients (a) and phase portraits and phase iteration diagrams for some representative points: $\varepsilon_1 = 0.1, \varepsilon_2 = 0.05$ (b), $\varepsilon_1 = 0.2, \varepsilon_2 = 0.1$ (c), $\varepsilon_1 = 0.2, \varepsilon_2 = 0.3$ (d), $\varepsilon_1 = 0.3, \varepsilon_2 = 0.5$ (e).

If the subsystems are decoupled, each of them manifests quasi-periodic oscillations. In the unified system it corresponds to the three-dimensional torus (T3), which persists as well at weak non-zero coupling. In a case of relatively strong coupling only in one of the subsystems, the coupling is sufficient to synchronize the partner subsystem, but no backward transmission of the oscillatory phase occurs. As a result, we observe regions of quasi-periodicity placed along the horizontal and vertical coordinate axes. For large ε_1 with increasing ε_2 the transition to hyperbolic chaos occurs through destruction of the quasi-periodicity. The transformation of the phase portraits and the phase iteration diagrams look like those illustrated in

Fig. 3. On the contrary, at high ε_2, between the regions of quasi-periodicity and hyperbolic chaos there is a band where the period doubling cascade occurs. More clearly, this scenario is illustrated in the next figure.

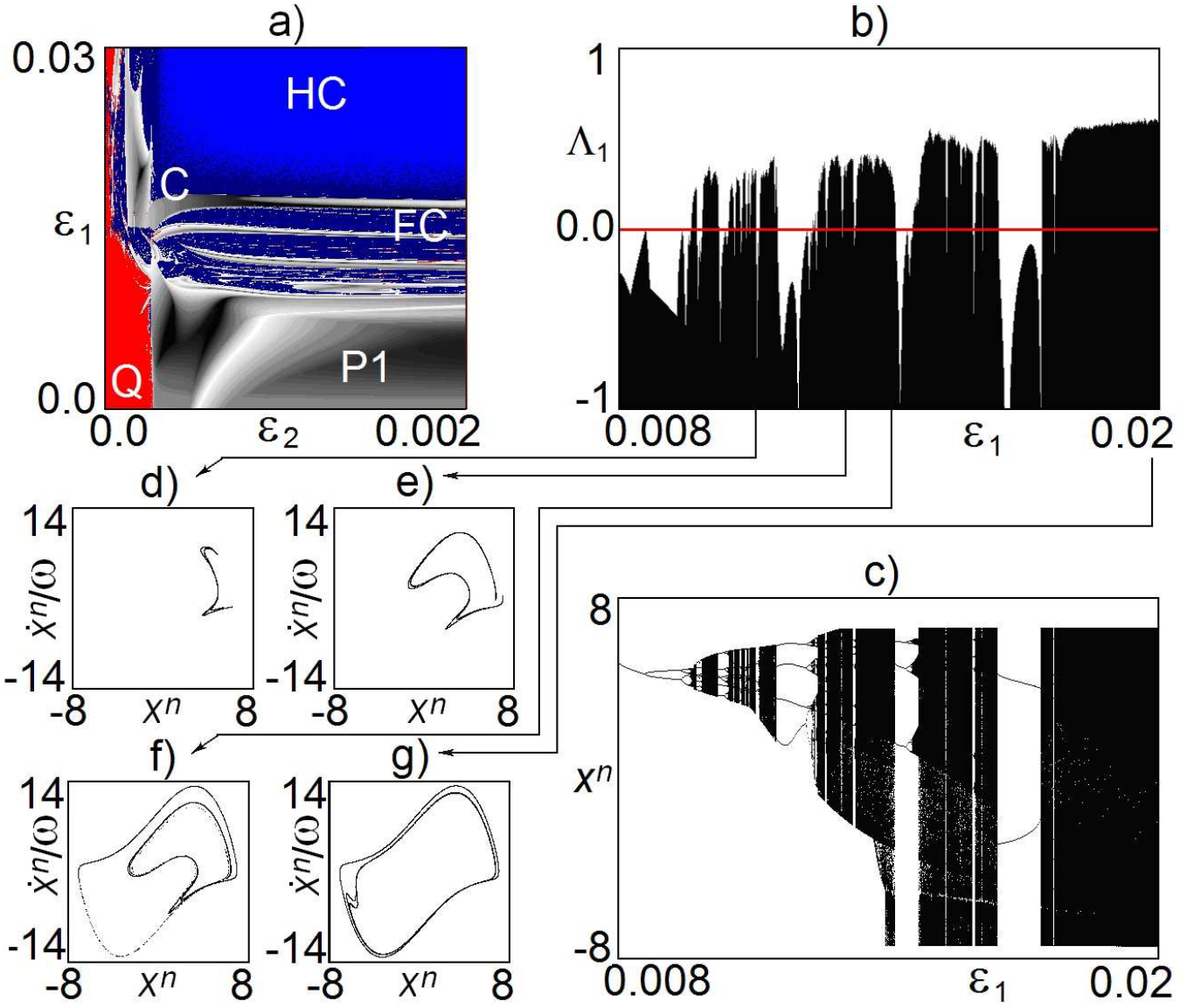

Fig. 6. Chart of dynamical regimes on the plane of coupling parameters for the model (1) with parameter values $A = 9.425, h_1 = 3.142, h_2 = 0.942$ (a), plot for the largest Lyapunov exponent (b) and bifurcation tree (c) versus the coupling coefficient ε_1 at fixed $\varepsilon_2 = 0.002$, and stroboscopic portraits of attractors at $\varepsilon_2 = 0.011$ (d), $\varepsilon_2 = 0.013$ (e), $\varepsilon_2 = 0.014$ (f), $\varepsilon_2 = 0.02$ (g).

By selecting values of the mean activity control parameters and of the amplitude of modulation it is possible to achieve a situation that the first subsystem without influence on the second one would demonstrate a resonant limit cycle instead of the torus. Then, we can observe on the plane $(\varepsilon_1, \varepsilon_2)$ a purified variant of the transition to the hyperbolic chaos preceded by the complete period-doubling bifurcation cascade; it takes place on roads upward in the right-hand part of Fig. 6. On the left side of the figure, like in the previously discussed case, the transition is accompanied with destruction of the quasi-periodicity.

The phase portraits in stroboscopic section (panels (d)-(g) in Fig. 6) demonstrate how the non-hyperbolic chaotic attractor, resembling the attractor in the Hénon map, becomes more and more de-

veloped. Gradually, it turns to a closed fractal set of loops, some of which cross the origin later, forming finally the Smale–Williams solenoid.

Panels (b) and (c) show, respectively, the plot of the largest Lyapunov exponent and the bifurcation tree diagram for the transition we discuss. Observe the period-doubling cascade and a wide region of non-rough chaos on the way to the hyperbolic attractor. The crown of the bifurcation tree in the respective parameter interval contains many windows of periodicity, where the Lyapunov exponent drops to negative values. As we can see the base periods of the widest windows increase from right to left each time by one. It is analogous to the phenomenon of period adding reported e.g. for piecewise linear systems [Kaneko, 1982; Maistrenko *et al.*, 1998; Pei *et al.*, 1986].

Concerning the diagrams in Fig. 5 and 6, it should be noted that the distinguishing between two kinds of non-rough chaos, the "destroyed torus" (C) and the "Feigenbaum attractor" (FC) is fairly conventional in nature, especially in the process of their transformation into the Smale–Williams solenoid. Indeed, compare the attractors in Fig. 5 (d) and Fig. 6 (f), which arise in the course of different scenarios, but are topologically similar each other. One can suppose that both described scenarios are actually interconnected.

3. Electronic experiment

It is interesting to observe the parameter space topography and the scenarios of transition to hyperbolic chaos in a real electronic experiment. For this purpose, departing from the earlier suggested schemes [Kuznetsov & Seleznev, 2006; Kuznetsov & Ponomarenko, 2008], on a base of more modern electronic components, we have built a laboratory device able to serve as a generator of hyperbolic chaos roughly corresponding to the mathematical model (1).

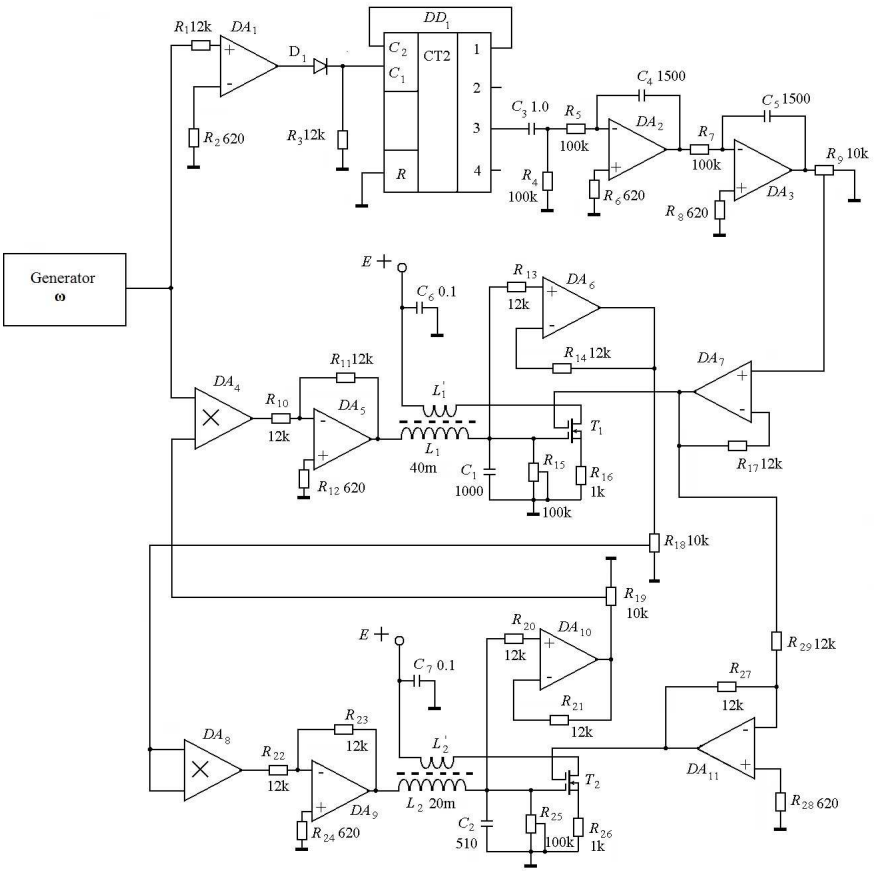

Fig. 7. Circuit diagram of the electronic generator of hyperbolic chaos. Frequency of the reference signal from the external generator is 24.5 kHz.

Schematic diagram of the circuit is shown in Fig. 7. It is composed of two partial self-oscillatory subsystems containing the inductor-capacitor circuits L_1C_1 and L_2C_2, supplemented by negative resistance elements arranged with the operational amplifiers DA_6 and DA_{10}. Dynamical variables x and y of the model (1) correspond in the experimental device to the voltages U_1 and U_2 across the capacitors C_1 and C_2. Quadratic coupling responsible for the transfer of excitation from the first oscillator to the second is provided by a multiplier DA_8 and an operational amplifier DA_9. The circuit containing the multiplier DA_4 and the operational amplifier DA_5 provides the effect of the second oscillator onto the first one via the product of the signal with the reference sinusoidal signal from generator of frequency close to the natural frequency of the first oscillator. Modulation of the activity in the subsystems in counter-phase is provided by variation of resistances of the field-effect transistors T_1 and T_2 controlled by signal from the frequency divider producing a sinusoidal voltage of period 8 times larger than the period of the reference signal. The amplitudes of parameter modulation in the subsystems can be regulated by the potentiometers R_{18} and R_{19}. The mean activity parameters of the subsystems are controlled by the potentiometers R_{15} and R_{25} determining a level of the resistive energy loss in the oscillatory circuits L_1C_1 and L_2C_2.

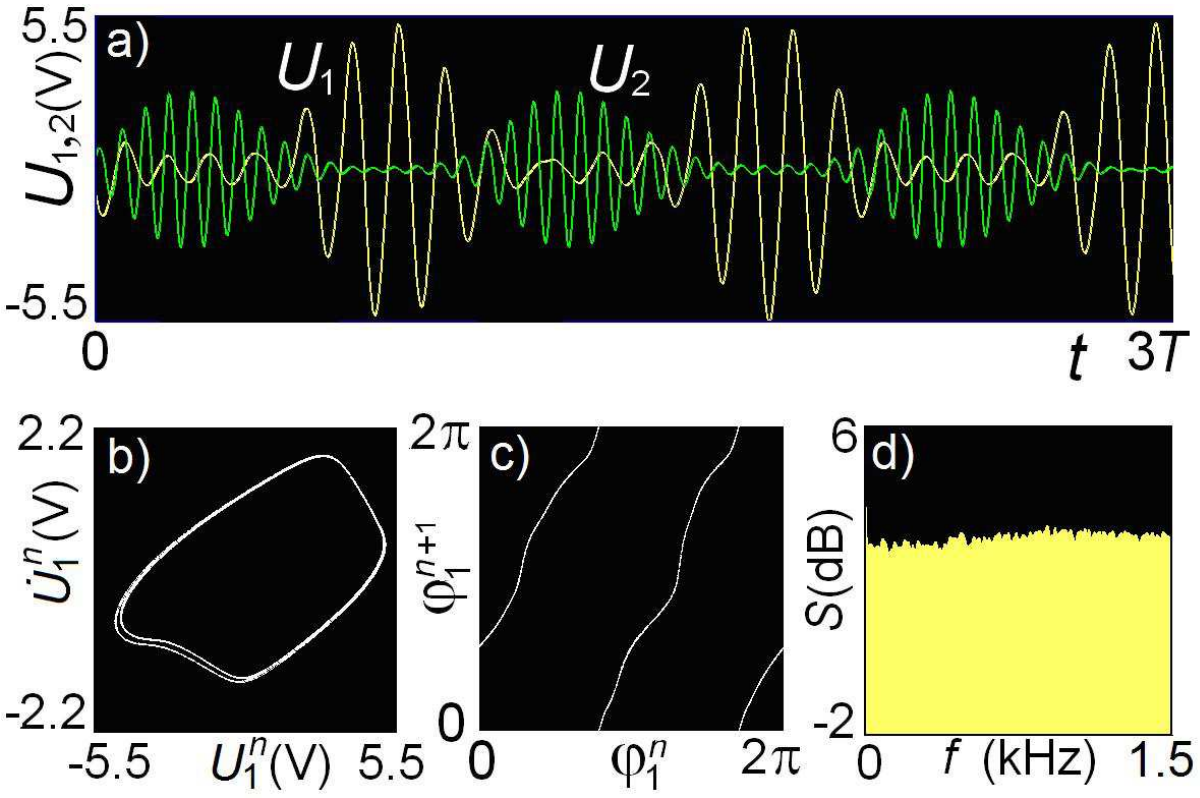

Fig. 8. The experimentally obtained typical samples of time dependences for voltages in the first and second subsystem in regime of hyperbolic chaos generation (a), respective stroboscopic portrait of attractor in the first subsystem (b), the iteration diagram for the phases on successive modulation periods (c) and the Fourier power spectrum of generated signal (d). The phases were computed from the recorded defined by the relation $\varphi = \arg[c(U_1/a + \dot{U}_1/b) + id(\dot{U}_1/b + U_1/a)]$ with empirically chosen constants $a = 5.5, b = 2.2, c = 0.7, d = 1.2$.

With appropriate settings of parameters it is possible to observe the hyperbolic chaotic dynamics like in the model (1). Fig. 8 shows typical samples of time dependences for the oscillating voltages in the first and the second subsystems (panel (a)). In the stroboscopic section corresponding to processing of a sequence of states following with the modulation period, chaotic attractor on the plane "voltage – current" certainly looks topologically equivalent to a projection of the Smale–Williams solenoid (panel (b)). The iteration diagram for phases of oscillations on successive stages of activity corresponds to the topology of the Bernoulli map (panel (c)). Fourier power spectrum is continuous and is characterized by roughly

constant spectral density in some frequency range (panel (d)).

By varying parameters of coupling between the subsystems in the experimental device, we have depicted a chart of dynamical regimes shown in Fig. 9. Types of dynamics in different domains on the parameter plane were detected by observing and visual recognizing pictures on the oscilloscope screen in the stroboscopic section supplied with quantitative analysis of the digitized time series records. As seen, the chart looks similar to that in Fig. 6. In the right-hand part of the chart, starting from regular oscillations of period-1, on a road upward the parameter plane (see the arrow marked 1) we observe the period-doubling bifurcation sequence (P1 & PD) following by the area of Feigenbaum chaos pierced by multiple narrow periodicity windows (FC), and then arrive in the domain of hyperbolic chaos (HC) corresponding to the Smale–Williams attractor. In the left-hand part corresponding to a relatively weak coupling effect of the second system to the first we see a domain of quasi-periodic behavior (Q), and moving to the right on the parameter plane (the arrow marked 2) observe transition to non-rough chaos (C) and then to the hyperbolic chaos (HC).

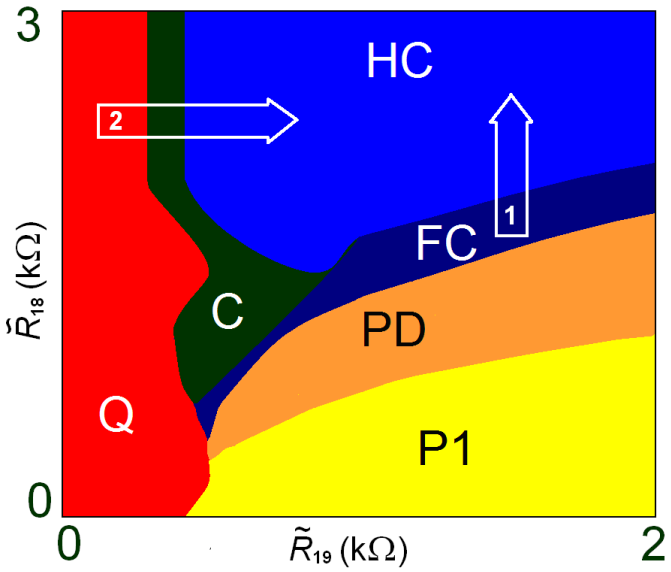

Fig. 9. Chart of dynamical regimes in the parameter plane of coupling resistances obtained for the experimental device. The arrows indicate two roads to hyperbolic chaos (HC): (1) via the Feigenbaum chaos (FC) resulting from the cascade of period doubling (PD) staring from the limit cycle of period 1 (P1) and (2) via chaotic regime (C) resulting from the destruction of the quasi-periodic dynamics (Q). The quantities counted along the coordinate axes are the variable parts of resistances of the potentiometers R_{18} and R_{19}, which are proportional to the parameters ε_1 and ε_2 of system (1) respectively.

Transformations of stroboscopic phase portraits and Fourier power spectra on the road 1 in the parameter plane chart are illustrated in Fig. 10. The diagram (a) relates to the chaotic attractor arisen via the period-doubling bifurcation cascade referred to as the Feigenbaum chaos; it is similar to attractor observed in the well-known Hénon map [Hénon, 1976; Devaney, 1989; Schuster & Just, 2005]. Power spectrum is continuous but it is notably non-uniform and contains high narrow peaks on the sides. The second picture (b) corresponds to intermittent chaotic regime that occurs nearby the most wide regularity window of period 3. The Fourier power spectrum shows pronounced peaks at 1/3 and 2/3 of the basic modulation frequency. The third diagram (c) relates to developed chaos, just before the transition to the hyperbolic attractor. The final transition from this Hénon-like attractor to the Smale–Williams solenoid occurs abruptly.

Stroboscopic phase portraits, iteration phase diagrams, and Fourier power spectra illustrating transition to hyperbolic attractor from quasi-periodic dynamics on the road 2 are shown in Fig. 11. In diagram (a) one can see an invariant curve representing the quasi-periodic attractor; the phase iteration map has in this case a single monotonous branch. Panel (b) shows formation of a singularity that is irremovable by variable changes; the iteration phase map becomes non-monotonous and locally non-invertible. Diagram (c)

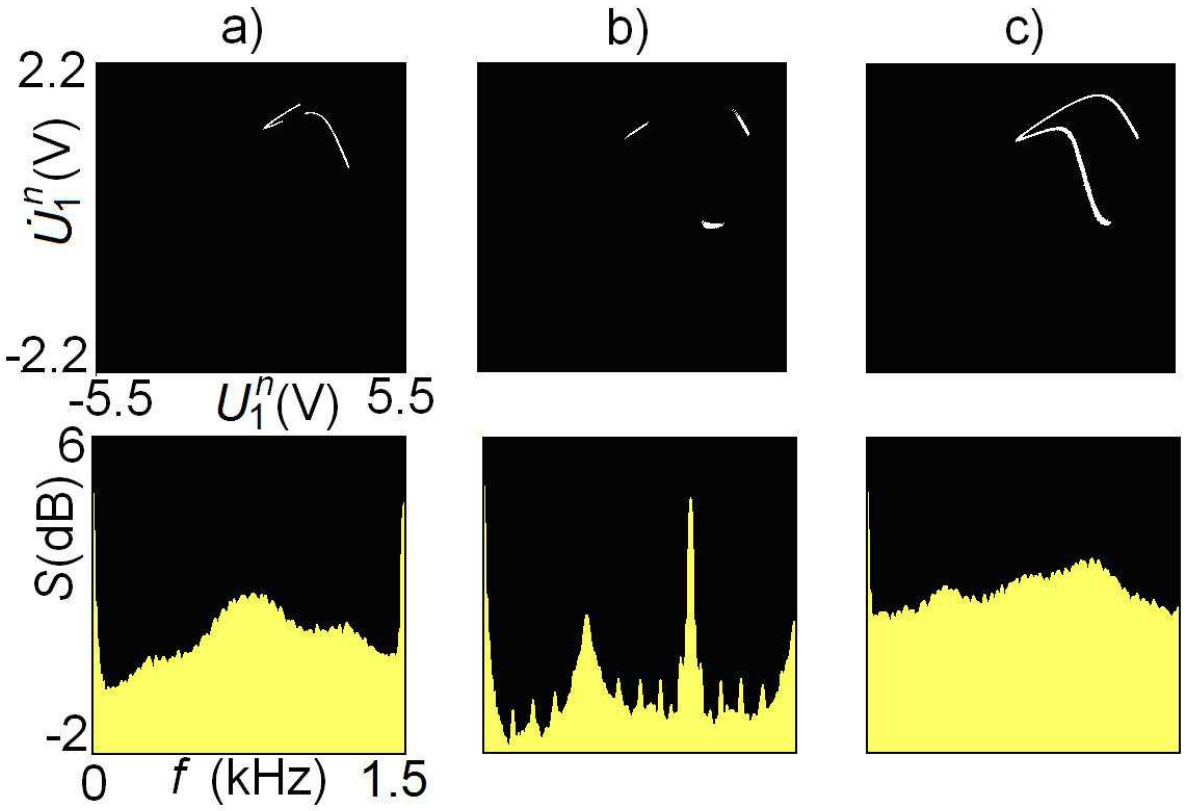

Fig. 10. Illustrations of transition to the hyperbolic chaos through Feigenbaum chaos on the road 1 on the parameter plane chart of Fig. 9. Stroboscopic portraits of the attractors and the Fourier power spectra are shown. Panel (a) corresponds to the Feigenbaum chaos arisen after the period-doubling cascade; panel (b) illustrates a regime of intermittency nearby the window of period 3 (b), and panel (c) relates to developed chaos, just before the transition to the hyperbolic attractor.

shows situation where the irreversibility is developing to a greater extent; the curve corresponding to the phase map tends to undergo a break there and to transform to the Bernoulli-type map with two branches. The Fourier power spectrum in the course of these transformations tends to smooth out.

4. Conclusion

For a particular non-autonomous system composed of two alternately excited self-oscillators capable to generate hyperbolic chaos we have examined disposition of different regular and chaotic regimes in the parameter space. Previously, such an analysis was not carried out; only individual points in the parameter space were studied and presence of the hyperbolic attractor, the Smale–Williams solenoid in the Poincaré map, was established. Now we present and interpret charts of dynamical behavior for regions surrounding the domain of hyperbolic chaos, which give impression of possible scenarios of its appearance.

In traditional understanding, there are three basic scenarios of transition to chaos in dissipative systems under variation of a control parameter; we emphasize that they relate to the emergence of non-hyperbolic strange attractors, which are not rough:

(i) transition to chaos through the Feigenbaum period doubling bifurcation cascade;
(ii) transition via the saddle-node bifurcation (collision and disappearance of a pair of stable and unstable fixed points or limit cycles) with the emergence of intermittency;
(iii) scenario involving quasi-periodic dynamics followed by its destruction and the emergence of chaos.

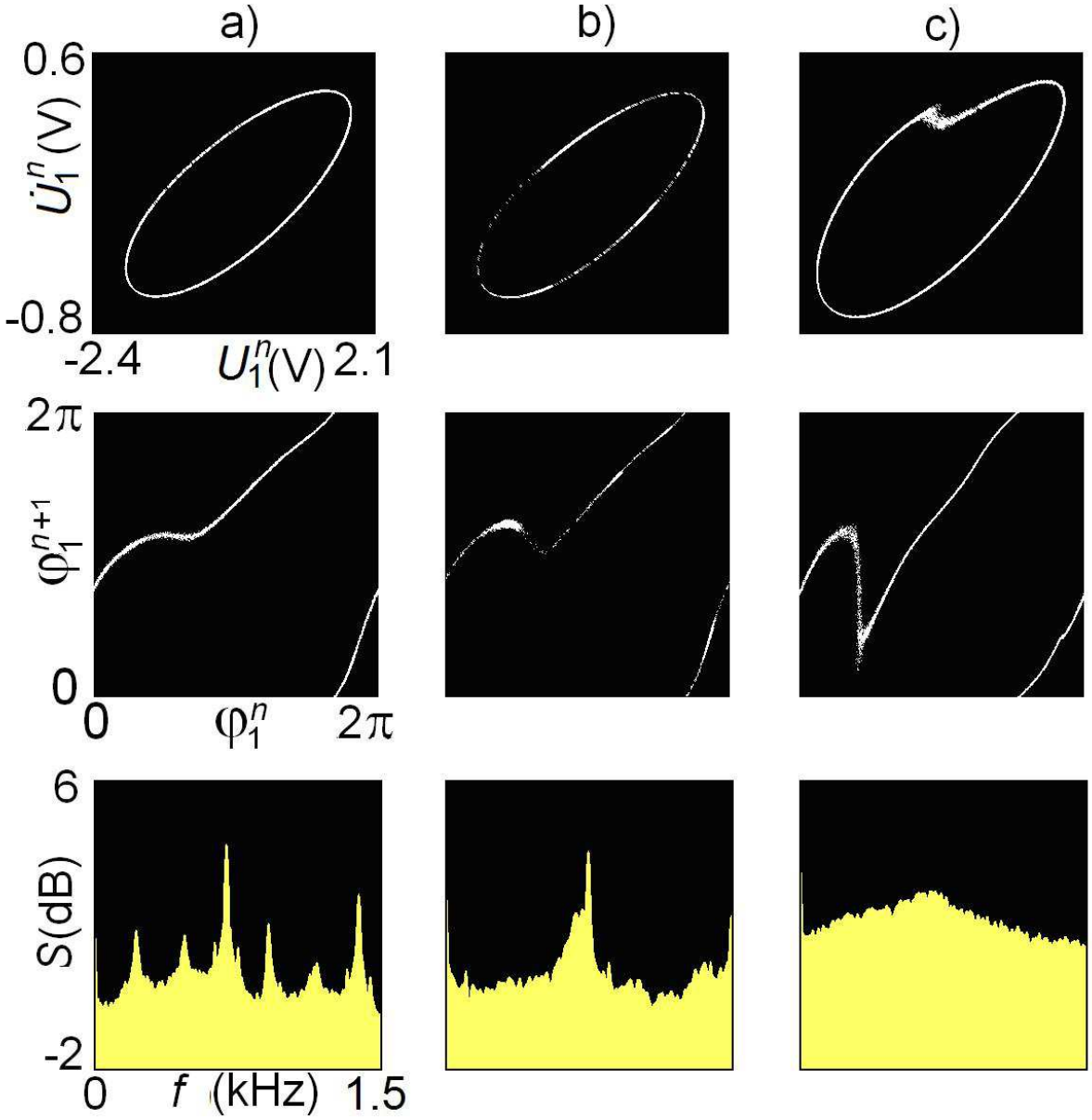

Fig. 11. Illustrations of transition to the hyperbolic chaos through destruction of quasi-periodicity on the road 2 on the parameter plane chart of Fig. 9. Stroboscopic portraits of the attractors, plots of iteration maps for phases at successive stages of activity and the Fourier power spectra are shown. Panel (a) corresponds to quasiperiodic attractor represented in the stroboscopic section by a closed invariant curve. Panel (b) illustrates appearance of singularity when the iteration phase map becomes irreversible. Panel (c) corresponds to situation just before the transition to the hyperbolic attractor. The phases were computed from the recorded defined by the relation $\varphi = \arg[c(U_1/a + \dot{U}_1/b) + id(\dot{U}_1/b + U_1/a)]$ with empirically chosen constants $a = 2.2, b = 0.7, c = 0.7, d = 1.8$.

Concerning origin of hyperbolic chaos associated with the Smale–Williams attractor, our study also indicates presence of three basic routes sketched in Fig. 12, which are in some analogy with the above listed classic scenarios.

One scenario of birth or destruction of hyperbolic chaos [Isaeva *et al.*, 2012, 2013] resembles a saddle-node bifurcation, but for the objects represented by sets of multiple orbits; one is the attractive Smale–Williams solenoid, and another is a solenoid with similar structure that is a non-attractive invariant set, a kind of chaotic saddle. The dynamics of the angular variable, characterizing instant states of the system, which belong to one or other involved solenoid, is governed by the doubly expanding circle map called the Bernoulli map. Hyperbolic chaos occurs in parameter domain where both involved invariant sets become

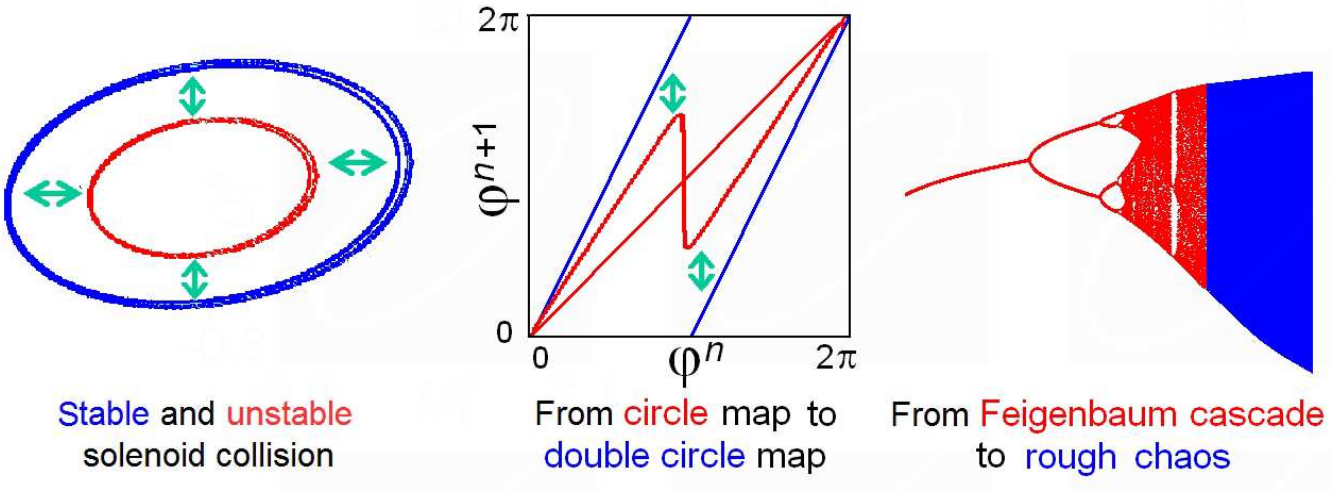

Fig. 12. A sketch of three ways of emergence of hyperbolic chaos.

separated. (It is opposite to the classic saddle-node scenario, where chaos occurs after annihilation of the involved objects, fixed points or limit cycles, with appearance of the Pomeau–Manneville intermittency [Bergé *et al.*, 1984].)

The second scenario relates to the transition from a situation where the dynamics on the attractor is quasi-periodic and corresponds to the circle maps for the angular variable with one branch in the graphical representation, to the situation of different topology, when the map has two branches. In the plane projection of the attractor the transition is accompanied with such transformation of curls representing the attractor that they cross the origin in such way that the mapping for the angular variable becomes doubly expanding and equivalent to the Bernoulli map.

The third scenario occurs in a situation when a departure from the region of hyperbolic chaos entails appearance of humps and hollows in the graph of the map for angular variable initially corresponding to the Bernoulli map. In the backward road in the parameter space towards the hyperbolic attractor, one can observe in this case a sequence of period-doubling bifurcations (due to the presence of the quadratic maxima and minima of the map for the angular variable) with subsequent transition to Feigenbaum chaos, which is non-rough (as the area is riddled with narrow windows of regular dynamics), and then to the hyperbolic chaos. It can be assumed that similar scenarios of the birth of hyperbolic chaos associated with attractors of Smale – Williams type may occur in other systems too. Perhaps, analogous scenarios may be found as well for the onset of other types of hyperbolic attractors. This question obviously deserves further deeper elaboration, both in the direction of consideration of other concrete examples and of development of generic models to refine general regularities inherent to each scenario.

Acknowledgments

This work was partially supported by RFBR grant No. 14-02-00085 and grant of the President of the Russian Federation for leading scientific schools NSH-1726.2014.2. D. V. S. acknowledges support from RFBR grant No. 14-02-31067.

References

Afraimovich, V. & Hsu, S.-B. [2003] *Lectures on chaotic dynamical systems* (International Press, Somerville, MA).

Andronov, A. A. & Pontryagin, L. [1937] "Systémes grossiers," *Dokl. Akad. Nauk. SSSR* **14**, 247–251.

Andronov, A. A., Vitt, A. A. & Khaikin, S. E. [1966] *Theory of oscillators* (Pergamon Press, Oxford).

Anosov, D. V. [1967] "Geodesic flows on closed riemannian manifolds of negative curvature," *Trudy Mat. Instit. Steklov* **90**, 3–210.

Anosov, D. V. (ed.) [1995] *Dynamical Systems IX: Dynamical Systems with Hyperbolic Behaviour*, Encyclopaedia of Mathematical Sciences, Vol. 66 (Springer, Berlin, Heidelberg).

Baptista, M. S. [1998] "Cryptography with chaos," *Phys. Lett. A* **240**, 50–54.

Baranov, S. V., Kuznetsov, S. P. & Ponomarenko, V. I. [2010] "Chaos in the phase dynamics of q-switched van der pol oscillator with additional delayed-feedback loop," *Izvestiya VUZ. Appl. Nonlin. Dynam. (Saratov)* **18**, 11–23, (In Russian).

Belykh, V., Belykh, I. & Mosekilde, E. [2005] "Hyperbolic plykin attractor can exist in neuron models," *Int. J. Bif. Chaos* **15**, 3567–3578.

Benettin, G., Galgani, L., Giorgilli, A. & Strelcyn, J.-M. [1980] "Lyapunov characteristic exponents for smooth dynamical systems and for hamiltonian systems; a method for computing all of them. part 1: Theory," *Meccanica* **15**, 9–20.

Bergé, P., Pomeau, Y. & Vidal, C. [1984] *Order within chaos* (John Wiley & Sons).

Devaney, R. L. [1989] *An introduction to chaotic dynamical systems* (Addison-Wesley, New York).

Dmitriev, A. S., Efremova, E. V., Maksimov, N. A. & Panas, A. I. [2012] *Generation of Chaos* (Tekhnosfera, Moscow), (In Russian).

Dmitriev, A. S. & Panas, A. I. [2002] *Dynamical Chaos: New Information Carriers for Communication Systems* (Fizmatlit, Moscow), (In Russian).

Eckmann, J.-P. [1981] "Roads to turbulence in dissipative dynamical systems," *Rev. Mod. Phys.* **53**, 643–654.

Elwakil, A. S. [2002] "Nonautonomous pulse-driven chaotic oscillator based on chua's circuit," *Microelectr. J.* **33**, 479–486.

Feigenbaum, M. J. [1983] "Universal behavior in nonlinear systems," *Physica D: Nonlin. Phenom.* **7**, 16–39.

Hénon, M. [1976] "A two-dimensional mapping with a strange attractor," *Comm. Math. Phys.* **50**, 69–77.

Hunt, T. [2001] "Low dimensional dynamics: bifurcations of cantori and realisations of uniform hyperbolicity," PhD thesis, University of Cambridge.

Hunt, T. J. & MacKay, R. S. [2003] "Anosov parameter values for the triple linkage and a physical system with a uniformly chaotic attractor," *Nonlinearity* **16**, 1499–1510.

Isaeva, O. B., Jalnine, A. Y. & Kuznetsov, S. P. [2006] "Arnold's cat map dynamics in a system of coupled nonautonomous van der Pol oscillators," *Phys. Rev. E* **74**, 046207.

Isaeva, O. B., Kuznetsov, S. P. & Mosekilde, E. [2011] "Hyperbolic chaotic attractor in amplitude dynamics of coupled self-oscillators with periodic parameter modulation," *Phys. Rev. E* **84**, 016228.

Isaeva, O. B., Kuznetsov, S. P. & Osbaldestin, A. [2007] "Complex analytic dynamics phenomena in a system of coupled nonautonomous oscillators with alternative excitation," *Tech. Phys. Lett.* **33**, 748–751.

Isaeva, O. B., Kuznetsov, S. P. & Osbaldestin, A. H. [2008] "A system of alternately excited coupled non-autonomous oscillators manifesting phenomena intrinsic to complex analytical maps," *Physica D: Nonlin. Phenom.* **237**, 873–884.

Isaeva, O. B., Kuznetsov, S. P. & Sataev, I. R. [2012] "A saddle-node bifurcation scenario for birth or destruction of a smale–williams solenoid," *Chaos: Interdisc. J. Nonl. Sci.* **22**, 043111.

Isaeva, O. B., Kuznetsov, S. P., Sataev, I. R. & Pikovsky, A. [2013] "On a bifurcation scenario of a birth of attractor of smale-williams type," *Nelineinaya Dinamika [Russian J. Nonlin. Dynam.]* **9**, 267–294, (In Russian).

Kaneko, K. [1982] "On the period-adding phenomena at the frequency locking in a one-dimensional mapping," *Progr. Theor. Phys.* **68**, 669–672.

Katok, A. & Hasselblatt, B. [1997] *Introduction to the modern theory of dynamical systems* (Cambridge University Press, Cambridge).

Koronovskii, A. A., Moskalenko, O. I. & Hramov, A. E. [2009] "On the use of chaotic synchronization for secure communication," *Physics-Uspekhi* **52**, 1213.

Kuptsov, P. V. [2012] "Fast numerical test of hyperbolic chaos," *Phys. Rev. E* **85**, 015203.

Kuznetsov, S. P. [2005] "Example of a physical system with a hyperbolic attractor of the smale-williams

type," *Phys. Rev. Lett.* **95**, 144101.
Kuznetsov, S. P. [2010] "Example of blue sky catastrophe accompanied by a birth of smale-williams attractor," *Reg. Chaot. Dynam.* **15**, 348–353.
Kuznetsov, S. P. [2011a] "Dynamical chaos and uniformly hyperbolic attractors: from mathematics to physics," *Physics-Uspekhi* **54**, 119–144.
Kuznetsov, S. P. [2011b] "Electronic circuits manifesting hyperbolic chaos and their simulation with software package multisim," *arXiv preprint arXiv:1111.5839* .
Kuznetsov, S. P. [2011c] "Plykin type attractor in electronic device simulated in multisim," *Chaos: Interdisc. J. Nonl. Sci.* **21**, 043105.
Kuznetsov, S. P. [2012] *Hyperbolic Chaos: A Physicist's View* (Higher Education Press, Beijing and Springer, Berlin, Heidelberg).
Kuznetsov, S. P. & Pikovsky, A. [2007] "Autonomous coupled oscillators with hyperbolic strange attractors," *Physica D: Nonlin. Phenom.* **232**, 87–102.
Kuznetsov, S. P. & Ponomarenko, V. I. [2008] "Realization of a strange attractor of the smale-williams type in a radiotechnical delay-feedback oscillator," *Tech. Phys. Lett.* **34**, 771–773.
Kuznetsov, S. P., Ponomarenko, V. I. & Seleznev, E. P. [2013] "Autonomous system generating hyperbolic chaos: circuit simulation and experiment," *Izvestiya VUZ. Appl. Nonlin. Dynam. (Saratov)* **21**, 17–30, (In Russian).
Kuznetsov, S. P. & Sataev, I. R. [2006] "Verification of hyperbolicity conditions for a chaotic attractor in a system of coupled nonautonomous van der pol oscillators," *Izvestiya VUZ. Appl. Nonlin. Dynam. (Saratov)* **14**, 3–29, (In Russian).
Kuznetsov, S. P. & Sataev, I. R. [2007] "Hyperbolic attractor in a system of coupled non-autonomous van der pol oscillators: Numerical test for expanding and contracting cones," *Phys. Lett. A* **365**, 97–104.
Kuznetsov, S. P. & Seleznev, E. P. [2006] "A strange attractor of the smale-williams type in the chaotic dynamics of a physical system," *J. Exp. Theor. Phys.* **102**, 355–364.
Liu, L., Hu, J., He, Z., Han, C., Li, H. & Li, J. [2011] "Chaotic signal reconstruction with application to noise radar system." *EURASIP J. Adv. Sig. Proc.* **2011**, 2.
Lukin, K. A. [2001] "Noise radar technology," *Telecomm. Radio Eng.* **55**.
Maistrenko, Y. L., Maistrenko, V. L. & Vikul, S. I. [1998] "On period-adding sequences of attracting cycles in piecewise linear maps," *Chaos, Solitons & Fractals* **9**, 67–75.
Newhouse, S., Ruelle, D. & Takens, F. [1978] "Occurrence of strange axioma attractors near quasi periodic flows on t^m, $m \geq 3$," *Comm. Math. Phys.* **64**, 35–40.
Pei, L.-Q., Guo, F., Wu, S.-X. & Chua, L. [1986] "Experimental confirmation of the period-adding route to chaos in a nonlinear circuit," *Circuits Syst., IEEE Trans.* **33**, 438–442.
Plykin, R. V. [1974] "Sources and sinks of a-diffeomorphisms of surfaces," *Math. USSR Sb.* **23**, 233.
Ruelle, D. & Takens, F. [1971] "On the nature of turbulence," *Comm. Math. Phys.* **20**, 167–192.
Schuster, H. G. & Just, W. [2005] *Deterministic chaos: an introduction* (John Wiley & Sons).
Shannon, C. E. [1948] "A mathematical theory of communication," *Bell System Tech. J.* **27**, 379–423.
Shil'nikov, L. P. [1997] "Mathematical problems of nonlinear dynamics: a tutorial," *International Journal of Bifurcation and Chaos* **7**, 1953–2001.
Shil'nikov, L. P., Shil'nikov, A. L., Turaev, D. V. & Chua, L. O. [1998] *Methods of qualitative theory in nonlinear dynamics* (Part 1), World Scientific Series on Nonlinear Science Series A, Vol. 4 (World Scientific, Singapore).
Shil'nikov, L. P., Shil'nikov, A. L., Turaev, D. V. & Chua, L. O. [2001] *Methods of qualitative theory in nonlinear dynamics* (Part 2), World Scientific Series on Nonlinear Science Series A, Vol. 5 (World Scientific, Singapore).
Shil'nikov, L. P. & Turaev, D. V. [1997] "Simple bifurcations leading to hyperbolic attractors," *Comp. Math. Appl.* **34**, 173–193.
Smale, S. [1967] "Differentiable dynamical systems," *Bull. Amer. Math. Soc.* **73**, 747–817.
Stojanovski, T. & Kocarev, L. [2001] "Chaos-based random number generators. part i: analysis," *Circuits and Systems I: Fundam. Theor. Appl., IEEE Trans.* **48**, 281–288.
Stojanovski, T., Pihl, J. & Kocarev, L. [2001] "Chaos-based random number generators. part ii: practical

realization," *Circuits and Systems I: Fundam. Theor. Appl., IEEE Trans.* **48**, 382–385.

Wilczak, D. [2010] "Uniformly hyperbolic attractor of the smale-williams type for a poincaré map in the kuznetsov system," *SIAM J. Appl. Dynam. Syst.* **9**, 1263–1283.

Williams, R. F. [1974] "Expanding attractors," *Publ. Math. de l'IHES* **43**, 169–203.

Yang, T. [2004] "A survey of chaotic secure communication systems," *Int. J. Comp. Cognition* **2**, 81–130.

Zhen, P., Zhao, G., Min, L. & Li, X. [2014] "A survey of chaos-based cryptography," *P2P, Parallel, Grid, Cloud and Internet Computing (3PGCIC), 2014 Ninth International Conference on* (IEEE), pp. 237–244.

Zhirov, A. Y. [2000] "Complete combinatorial invariants for conjugacy of hyperbolic attractors of diffeomorphisms of surfaces," *J. Dynam. Control Syst.* **6**, 397–430.